# Enabling Underwater Acoustic Cooperative MIMO Systems by Metamaterial-Enhanced Magnetic Induction

Soham Desai<sup>1</sup>, Vaishnendr D Sudev<sup>1</sup>, Xin Tan<sup>1</sup>, Pu Wang<sup>2</sup>, and Zhi Sun<sup>1</sup>

<sup>1</sup>Dept. of Electrical Engineering, State University of New York at Buffalo, Buffalo NY 14260

<sup>2</sup>Dept. of Computer Science, University of North Carolina at Charlotte, Charlotte, NC, 28223

E-mail: <sup>1</sup>{sohamdhi, vaishnen, xtan3, zhisun}@buffalo.edu, <sup>2</sup>Pu.Wang@uncc.edu

Abstract—The acoustic cooperative multi-input-multi-output (MIMO) systems equipped on the underwater robot swarms (URSs) can enable long-range and high-throughput communications. However, the acoustic communications cannot provide the real-time and accurate synchronization for the distributed transmitters of the cooperative MIMO due to the large delay of acoustic channels. In addition, the narrow bandwidth of the acoustic channel further enlarges the synchronization time and errors. In this paper, we propose the metamaterial magnetic induction (M<sup>2</sup>I)-assisted acoustic cooperative MIMO to address aforementioned challenges. The synchronization time can be reduced since the M<sup>2</sup>I has negligible signal propagation delays. To quantitatively analyze the improvement, we deduce the synchronization errors, signal-to-noise ratio (SNR), effective communication time, and the throughput of the system. Finally, the improvement of using M<sup>2</sup>I-assisted synchronization is validated by the numerical evaluation.

#### I. Introduction

Recent advances in computation, communication, control and robotics have paved the way to realize and deploy underwater robot swarms (URSs) [1], [2], [3]. Unlike distributed underwater robotic systems in general, the URS can timely and effectively accomplish the complex missions by exploiting the collective intelligence that emerges from the local interactions among the robots. This requires reliable and real-time communications among the robots within a swarm. Moreover, many underwater missions require long-range and high-throughput communications between the robot swarm and the remote base station. However, due to the harsh underwater environments, none of the existing wireless networking techniques can simultaneously satisfy the above requirements.

The underwater acoustic multi-input-multi-output (MIMO) system may be used to satisfy the long-range and high-throughput requirements [4]. However, the size of underwater robots is of the same order of the acoustic wavelength in water (tens of centimeters). As a result, it is impractical to place multiple acoustic transponders in the same underwater robots with enough interspace to guarantee the spatial independence (usually more than half wavelength). Moreover, even with MIMO, a single robot still has the limited communication range because of its limited on-board power source.

To address aforementioned problems, the cooperative MIMO can be utilized, which is well developed for terrestrial

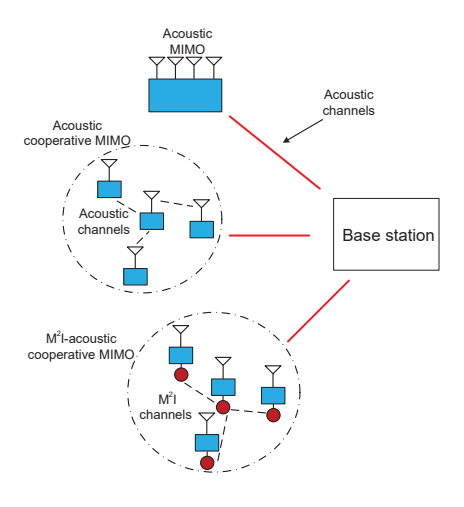


Fig. 1. The concept of M<sup>2</sup>I-acoustic cooperative MIMO systems.

wireless systems [5]. By forming an virtual antenna array using multiple agents, cooperative MIMO can sufficiently increase the range of wireless links, while saving the energy of each transmitting agent. As shown in Fig. 1, instead of equipping multiple transmitters on one robot, each robot carries an antenna so that the cooperative MIMO is realized by deploying a cluster of robots. As a result, the signal-tonoise ratio (SNR) or channel capacity can be enhanced to have long-range and hight-throughput communications. However, the cooperative MIMO system requires real-time communications among the robots to synchronize the transmitters. The large-delay acoustic channels among the robot swarm cannot satisfy the synchronization requirements since it takes long synchronization time and has large synchronization errors. To address the problem, we propose the acoustic cooperative MIMO system assisted by metamaterial enhanced magnetic induction (M<sup>2</sup>I) communications [6]. The M<sup>2</sup>I-based communication has negligible signal propagation delay because the electromagnetic waves have an underwater propagation speed of  $3.33 \times 10^7$  m/s. Such extremely high-speed signal propagation can significantly improve the delay performance, while facilitating the synchronization of the distributed transmitters. In addition, the power enhancement achieved by the metamaterial enlarges the communication range among the

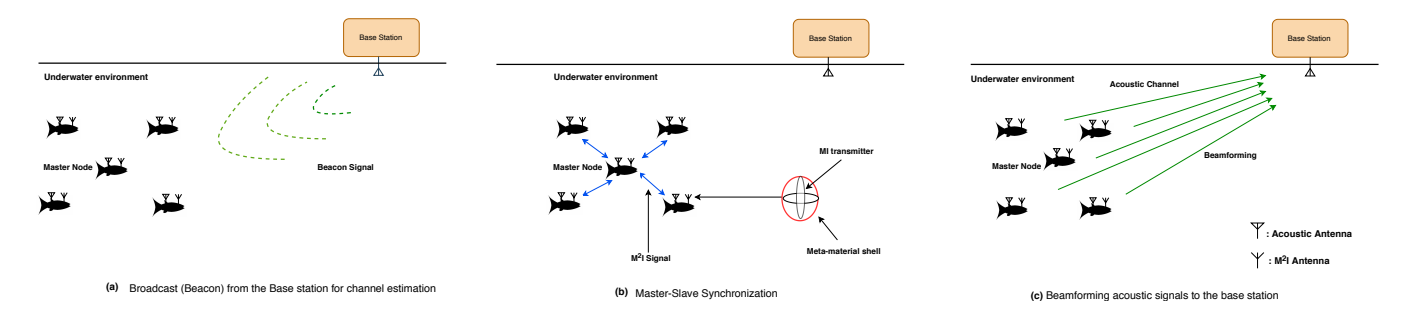


Fig. 2. The system architecture and scheduling of the M<sup>2</sup>I-acoustic cooperative MIMO.

robot swarm.

In this paper, we first propose the system architecture of the M<sup>2</sup>I-acoustic cooperative MIMO. By considering the synchronization time and clock drift, the time and frequency synchronization errors are calculated. Based on the synchronization errors, we analyze the communication performance of the acoustic cooperative MIMO, including SNR, and an upper bound of the throughput. Then, we evaluate the communication performance by comparing the pure acoustic-based synchronization and the M<sup>2</sup>I-assisted synchronization.

The remainder of this paper is organized as follows. The system architecture and scheduling is proposed in Section II. The Cooperative MIMO Synchronized by M<sup>2</sup>I and acoustic beamforming is discussed in Section III. The time and frequency synchronization errors are calculated and analyzed in Section IV. Based on the synchronization errors, the communication performance is analyzed in Section V. Then, the communication performance is evaluated by the numerical analysis in Section VI. Finally, the paper is concluded in Section VII.

#### II. SYSTEM ARCHITECTURE AND SCHEDULING

The M<sup>2</sup>I-acoustic cooperative MIMO aims to establish longrange and high throughput links between the robot swarm and the surface station by addressing the unreliable and highenergy consumption problems in existing underwater acoustic communication systems, especially in shallow and complex underwater environments, such as rivers and lakes. The system architecture and scheduling of the underwater cooperative MIMO is proposed as Fig. 2. A base station (BS) is located on the water surface for the data acquisition. The robot swarm is deployed for the detection and exploitation tasks in the underwater environment. To concert the distributed transmitters, a master node is chosen from the robot swarm and the others work as the slave node. For example, to transmit using either beamforming or space-time coding, the master node delivers the information by broadcasting so that each slave node gets a copy of the data. Moreover, the local hardware clock of the master node is used as the reference to synchronize slave nodes. For the beamforming communications, the channel state information (CSI) of the master node also needs be delivered to the slave nodes to compute the beamforming codebook.

The M<sup>2</sup>I-acoustic cooperative MIMO consists of two modules: the acoustic MIMO module and the M<sup>2</sup>I-assisted synchronization module. The acoustic MIMO module is achieved by concerting a cluster of distributed transmitters on the robot swarm. As mentioned, this distributed design can address the problems of the spatial and power source limitations to achieve long communication range with high throughput. However, the large-delay acoustic channels cannot satisfy the real-time synchronization requirements. The M<sup>2</sup>I-assisted synchronization modules are therefore designed to address the problem.

The  $M^2I$ -assisted synchronization module is mainly based on the tri-dimensional magnetic induction (MI) transceivers [7] and the metamaterial shells. The MI techniques have inherent advantages for wireless communications in lossy media, especially underwater [7]. In addition, the tri-dimensional design of the MI transceivers enables the tri-dimensional signal coverage. The metamaterial shell is developed to overcome the inefficient-antenna problem of the MI. By matching the negative permeability  $\mu$  of the metamaterials with the positive  $\mu$  of the environments, a resonant status of the entire antenna structure can be created. Therefore, the signal transmitted from the MI transmitters can be enhanced to provide sufficient communication range among the robot swarms.

The scheduling of the system comprises of a three-step process. In order for the nodes to beamform towards a remote BS, each source node needs to estimate its channel with respect to this BS. Hence, the BS broadcasts a beacon signal (e.g., a sinusoidal signal at the carrier frequency) as seen in Fig. 2-(a), using this signal the complex channel is estimated at every node. On receiving the beacon signal, the master and slave nodes use M<sup>2</sup>I antennas to synchronize their clocks as seen in Fig. 2-(b). Finally, all the nodes transmit acoustic signals towards the BS and act as a distributed beamformer as seen in Fig. 2-(c) [8].

## III. THE COOPERATIVE MIMO SYNCHRONIZED BY M<sup>2</sup>I COMMUNICATIONS AND ACOUSTIC BEAMFORMING

To enable the underwater cooperative MIMO systems, the distributed transmitters need to be synchronized in the underwater environments. The synchronization strategies for distributed transmitters can be classified as closed-loop synchronization and open-loop synchronization. For most of the closed-loop synchronization strategies, such as 1-bit-feedback

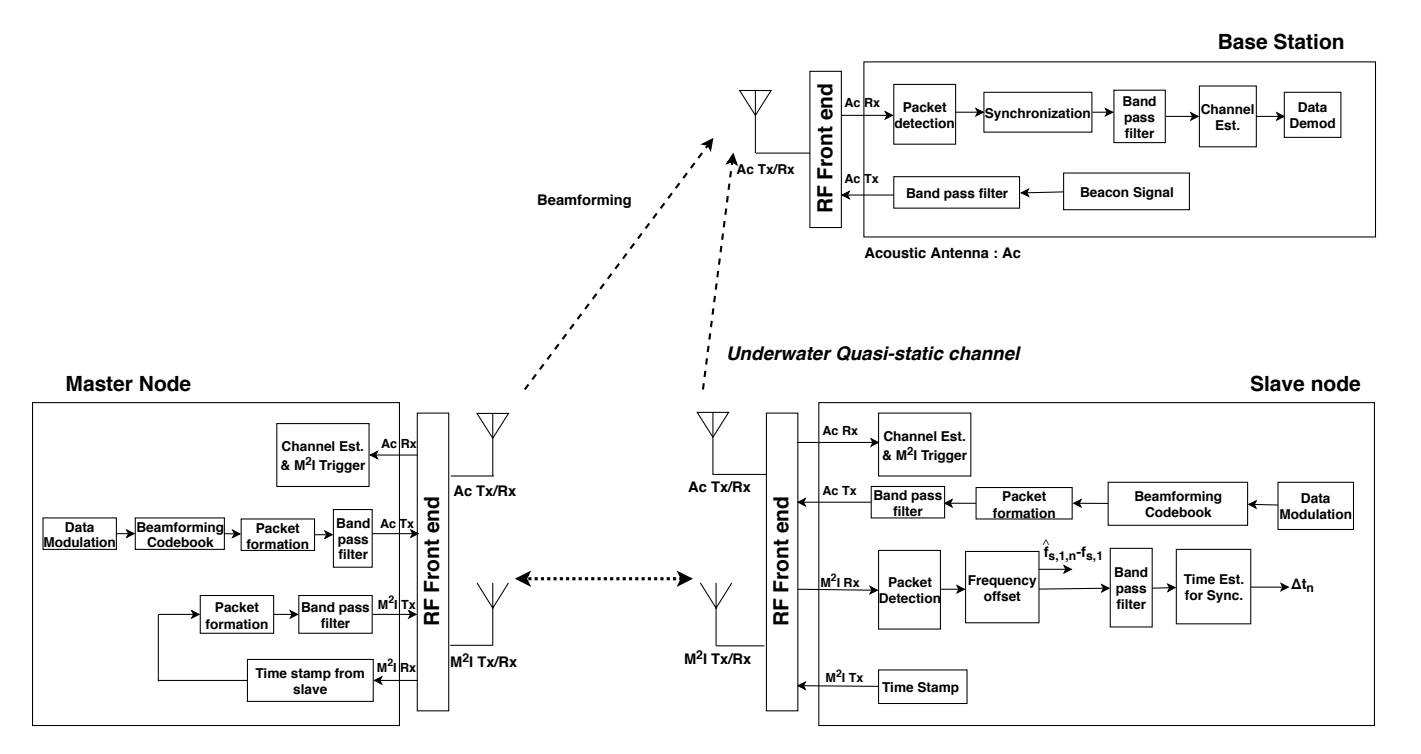


Fig. 3. The system model of underwater Cooperative M<sup>2</sup>I based acoustic MIMO.

synchronization and opportunistic-feedback synchronization, multiple rounds of feedback are required from the base station to converge the frequency and time offset [9]. However, due to the large delay of the acoustic channel between the base station and the transmitting nodes, the closed-loop synchronization based on the feedback cannot be applied in the underwater scenario. Therefore, we choose to use the master-slave synchronization based on the inter-node communication among transmitters [10], [11].

As shown in Fig. 4, the open-loop synchronization works as follows. A master node is predetermined from the transmitting nodes randomly and the other nodes can use the master node as the reference. The slave nodes visit the master node one by one to adjust their own local clock, the order in which they visit the master node is also predetermined. Since all the nodes have the same characteristics and M<sup>2</sup>I antennas used for synchronization have a relatively small delay, the assignment of the master and order of the slave nodes visiting the master node will not have an impact on the overall system performance. For each slave node, a time stamp generated by the local clock is delivered to the master node. Having received the time stamp, the master node generates the feedback, including the beacon signal, its own CSI and time stamp to the slave nodes. On receiving this feedback, the M<sup>2</sup>I receiver at the slave nodes detects the packet, estimates its frequency and time offset as in Fig. 3. The time offset is estimated using the time stamp received and the frequency offset is estimated by auto correlating the known beacon signal to the one received from the master node. The calculated offsets are utilized for synchronization. Compared to the acoustic

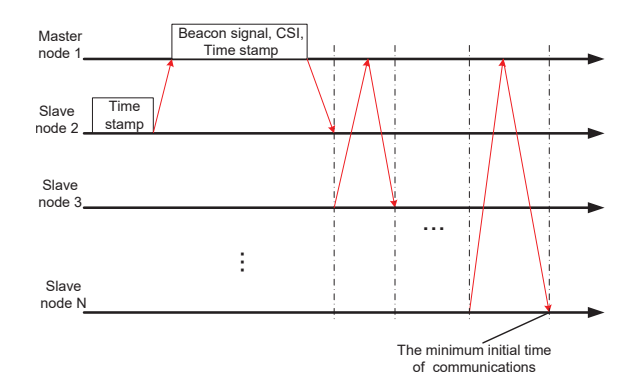


Fig. 4. The master-slave synchronization of underwater cooperative MIMO systems

channels, the M<sup>2</sup>I channels between the transmitting nodes have a very tiny delay. As a result, the synchronization time can be reduced and therefore the synchronization accuracy is significantly increased. The numerical analysis is formulated in section IV.

Further, when the synchronization is completed all the transmitting nodes beamform the data towards the BS. The working of this can be seen in the acoustic Tx nodes in Fig. 3. The modulated data is added with appropriate headers and a packet is formed. To perform beamforming, optimum phase control is applied and then through a band pass filter the data is transmitted towards the destination. The BS on receiving the packets, identifies the start of packet, performs synchronization and the original data is retrieved.

#### IV. ANALYSIS OF THE SYNCHRONIZATION ACCURACY

First, we analyze the frequency error of the synchronization. Considering the difference of the independent crystal oscillators in the transmitter nodes, the average relative clock drift of the n-th node to the master node in the time  $\Delta T$  can be presented as:

$$\bar{a}_n = \frac{\int_{\Delta T} a_n(t)dt}{\Delta T},\tag{1}$$

where  $a_n(t)$  is the time-varying drift defined as the ratio of oscillator frequencies:

$$a_n(t) = \frac{f_{c,n}(t)}{f_{c,1}(t)}. (2)$$

The subscript n = 2, 3, ..., N indicates the slave nodes. The subscript 1 indicates the master node.

For a certain transmitting node, the operating frequency  $f_{s,i}(t)$  is proportional to its hardware oscillator:

$$f_{s,i}(t) = k \cdot f_{c,i}(t) \quad \forall i = 1, 2, ...N,$$
 (3)

where k is the frequency multiplier. The frequency of the beacon signal generated by the master node is  $f_{s,1}$ . After receiving the beacon signal at the slave node n, the frequency is estimated according to the local oscillator of the slave node:

$$\hat{f}_{s,1,n} = \bar{a}_n f_{s,1} + \epsilon_{s,n},\tag{4}$$

where  $\epsilon_{s,n}$  is the error of the frequency estimation. Obviously, the frequency estimated by the slave node n  $\hat{f}_{s,1,n}$  is different from the transmitting frequency  $f_{s,1}$  due to the relative clock drift and the estimation error. Meanwhile, the slave node is told by the master node that the frequency of the beacon signal is  $f_{s,1}$ . Therefore, the difference of the frequency can be expressed as:

$$\hat{f}_{s,1,n} - f_{s,1} = (\bar{a}_n - 1)f_{s,1} + \epsilon_{s,n}. \tag{5}$$

The frequency offset at the slave node n for the frequency synchronization can be determined as:

$$\Delta f_{c,n} = \frac{\hat{f}_{s,1,n} - f_{s,1}}{k} = (\bar{a}_n - 1)f_{c,1} + \frac{\epsilon_{s,n}}{k}.$$
 (6)

According to (6), the optimal frequency offset is  $(\bar{a}_n - 1)f_{c,1}$ . Due to the estimation error  $\epsilon_{s,n}$ , the frequency cannot be perfectly synchronized and the error can be defined as:

$$\epsilon_{n,f} = \frac{\epsilon_{s,n}}{k}.\tag{7}$$

Then, we analyze the time error of the synchronization. Due to the clock drift caused by the difference of oscillators, the accuracy of both time and frequency synchronization decreases as the drift bound increases. Once the master node generates its time stamp to slave node n for the time synchronization, their clocks begin to relatively drift so that they will not start the beamforming at exactly the same time. According to the polling operation shown in Fig. 4, the duration of the time slot for the n-th node is calculated by:

$$\Delta t_n = \frac{L_{n,1} + L_{1,n}}{B} + \frac{2d_{1,n}}{c},\tag{8}$$

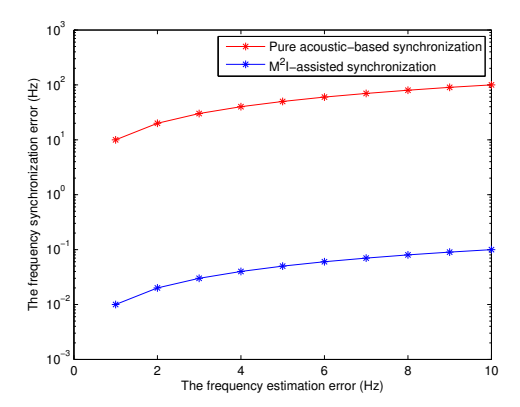


Fig. 5. The frequency synchronization error.

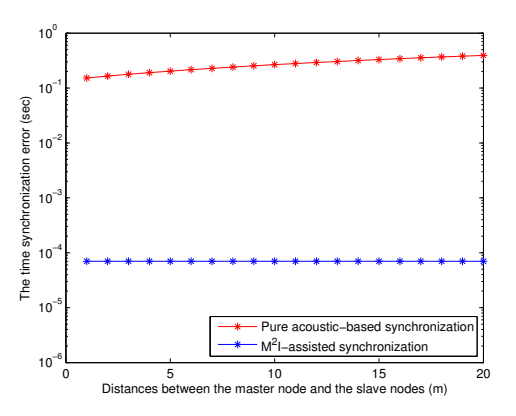


Fig. 6. The time synchronization error.

where  $L_{n,1}$  and  $L_{1,n}$  are the total packet length delivered from the slave node to the master node and that from the master node to the slave node, respectively. B is the bandwidth.  $d_{1,n}$  is the distance between the master node and the slave node n. c is the propagation speed of the signals. Obviously, compared to the acoustic channel, the  $M^2I$  channel has the larger bandwidth and propagation speed. Hence, the duration of each time slot can be reduced if the  $M^2I$  communication is utilized.

The total drifting time for the slave node n is computed from the timing that the master node generates the time stamp for node n to the earliest beamforming time  $t_{BF}$ . Considering the time of the master node as the reference, the time synchronization error of slave node n can be derived according to (7) and (8):

$$\epsilon_{n,t} = \epsilon_{n,f} \left( \frac{L_{1,n}}{B} + \frac{d_{1,n}}{c} + \sum_{i=n+1}^{N} \Delta t_i \right).$$
 (9)

Then we evaluate the frequency and time synchronization error in Fig. 5 and Fig. 6. The operating frequency is set to be 10 KHz for acoustic-assisted synchronization and 10 MHz for M<sup>2</sup>I-assited synchronization. The frequency of the crystal oscillator is 100 kHz. The number of transmitting nodes including the master node is 10. The distance between the slave nodes and master node are set to be 20 meters.

The packet length  $L_{n,1} = 100$  bits and  $L_{1,n} = 200$  bits. The bandwidth is set to be 10 kHz for acoustic channels and 20 kHz for M<sup>2</sup>I channels. As shown in Fig. 5, the frequency error is evaluated by considering the variation of the frequency estimation errors. Since the M<sup>2</sup>I-assisted synchronization uses higher frequency to synchronize the local hardware clock with lower frequency, the error will be much lower than that of pure acoustic-based synchronization. As shown in Fig. 6, the time synchronization error by considering acoustic communications is extremely high since the delay of the acoustic signals enlarges the drifting time. Shown as the blue curve, the time synchronization error can be reduced significantly once the  $M^2$ I-assisted synchronization is used.

### V. Performance Analysis of Using M<sup>2</sup>I-Assisted Synchronization

The signal transmitted on baseband is a train of raised cosine, bearing modulated symbols m(t). The received signal through the acoustic channel from one transmitter can be expressed in time domain:

$$r(t) = m(t)e^{j2\pi f} \sum_{p=1}^{N_{pa}} \frac{1}{\sqrt{P_{att}(f, d_p)}} e^{-j2\pi f \tau_p} + n(t),$$
 (10)

where f is the carrier frequency and n(t) is the noise. The time-invariant channel is considered within the synchronization time interval.  $N_{pa}$  is the number of paths.  $\tau_p$  is the propagation delay of the p-th path.  $P_{att}(f,d_p)$  is the channel attenuation depending on the distance  $d_p$  and the frequency f:

$$P_{att}(f, d_p) = \xi_p d_p^{\beta} e^{\alpha(f)d_p}, \tag{11}$$

where  $\xi$  is the scattering loss.  $d_p^{\beta}$  is the geometric spreading loss determined by the distance  $d_p$  and the spreading exponent  $\beta$ .  $\alpha(f)$  is the absorption coefficient. By considering the cooperative MIMO with N perfectly synchronized transmitters, the received signal can be written as:

$$r_N(t) = m(t)e^{j2\pi f} \sum_{i=1}^{N} \sum_{p=0}^{N_{pa,i}} \frac{1}{\sqrt{P_{att,p,i}(f,d_p)}} e^{-j2\pi f \tau_{p,i}} + n(t), \quad (12)$$

where the subscript i indicates the i-th transmitter. By considering the uniform distributed channel delay  $\tau_{p,i} \in [-\pi, \pi)$ , (12) can be simplified to:

$$r'_{N}(t) = \sum_{i=1}^{N} A e^{j2\pi f t} h_{i} e^{-j2\pi f \tau_{i}} + n(t),$$
 (13)

where A is the amplitude of the transmitted signal.  $h_i$  is the channel envelope that follows the PDF [12]:

$$p_{h_i}(z) = 4\pi^2 z \int_0^\infty \prod_{p=1}^{N_{pa,i}} J_0(2\pi |h_{p,i}|x) J_0(2\pi zx) J_0(2\pi h_{0,i}x) x dx,$$
(14)

where  $h_{p,i}$  is the channel attenuation of the *p*-th path for the transmitter *i*:

$$h_{p,i} = \frac{1}{\sqrt{P_{att,p,i}(f,d_p)}}. (15)$$

 $J_0(x)$  is developed as:

$$J_0(x) = \frac{1}{2\pi} \int_0^{2\pi} e^{jx\cos\beta} d\beta. \tag{16}$$

By considering the perfect CSI information, the channel envelope  $h_i$  and the delay  $\tau_i$  are known.

The underwater cooperative MIMO is developed for either beamforming or space-time coding. First, we analyze the performance of the beamforming by considering M<sup>2</sup>I/acoustic-based synchronization. The maximum SNR beamforming is considered in this case. The received signal after the phase control can be written as:

$$r_{N,BF}(t) = \sum_{i=1}^{N} A e^{j2\pi f t} h_i e^{-j2\pi f \tau_i} e^{j\phi_i} + n(t),$$
 (17)

where  $\phi_i$  is the phase control at the *i*-th transmitter. The objective of the beamforming is to align the phase and maximize the SNR at the receiver side. Therefore, the optimal phase control vector  $\mathbf{v}_{\phi}$  can be obtained by maximizing the SNR:

$$\max_{\mathbf{v}_{\phi}} \frac{A^2 \left| \mathbf{h}^{\mathsf{T}} \mathbf{v}_{\phi} \right|^2}{\sigma^2}, \tag{18}$$

where

$$\mathbf{h} \triangleq [h_1 e^{j2\pi f(t-\tau_1)} \ h_2 e^{j2\pi f(t-\tau_2)} \ \dots \ h_N e^{j2\pi f(t-\tau_N)}],$$

$$\mathbf{v}_{\phi} \triangleq [e^{j\phi_1} \ e^{j\phi_2} \ \dots \ e^{j\phi_N}], \qquad \sigma^2 \triangleq \mathbb{E}\{|n(t)|^2\}.$$
(19)

By considering the optimal phase control, the channel delay can be compensated by the phase control and the SNR at the received side can be maximized as:

$$SNR_{BF} = \frac{A^2 \left| \sum_{i=1}^{N} h_i \right|^2}{\sigma^2}.$$
 (20)

According to the synchronization error analysis presented in Section IV, the received signal can be expressed by considering the frequency and time errors:

$$r_{N,BF,\epsilon}(t) = \sum_{i=1}^{N} Ah_i e^{j2\pi(f+\epsilon_{i,f})(t-\tau_i+\epsilon_{i,t})} e^{j\phi_i} + n(t), \qquad (21)$$

where the  $\epsilon_{i,t}$  and  $\epsilon_{i,f}$  are respectively the time and frequency error of the *i*-th node. i=1 indicates the master node. Therefore we have  $\epsilon_{1,t}=0$  and  $\epsilon_{1,f}=0$ . The phase controlled SNR by considering the time and frequency error can be written as:

$$SNR_{BF,\epsilon}(t) = \frac{A^2 \left| \sum_{i=1}^{N} h_i e^{j2\pi(f + \epsilon_{i,f})(t + \epsilon_{i,t})} \right|^2}{\sigma^2}.$$
 (22)

Similarly, the maximum SNR and error considered SNR for the space-time coding can be represented by:

$$SNR_{SPTC} = \frac{A^2 \sum_{i=1}^{N} h_i^2}{\sigma^2},$$

$$SNR_{SPTC,\epsilon}(t) = \frac{A^2 \sum_{i=1}^{N} \left| h_i^2 e^{j2\pi(f + \epsilon_{i,f})(t + \epsilon_{i,t})} \right|}{\sigma^2}.$$
(23)

Due to the relative clock drift, the SNR presented in (20) and (23) will decrease with time. To maintain the communication,

the SNR is required to be greater than the threshold  $\eta$ . Once the SNR is about to be lower than the threshold, another round of synchronization is required. The effective communication time is defined as the duration between two adjacent rounds of synchronization that can be used to transmit useful information. Therefore, the effective communication time for the beamforming and space-time coding  $t_{BF,SNR}$ ,  $t_{SPTC,SNR}$  according to the SNR is constrained by:

$$t_{BF,SNR} = \min_{t} t$$
s.t.  $SNR_{BF,\epsilon}(t) < \eta$ , (24)

$$t_{SPTC,SNR} = \min_{t} t$$
s.t.  $SNR_{SPTC,\epsilon}(t) < \eta$ . (25)

Since the channel model is assumed to be quasi-static, the effective communication time cannot be greater than the coherence time defined as [13]:

$$T_c = \sqrt{\frac{9}{16\pi f_d^2}} \approx \frac{0.423}{f_d} = \frac{0.423}{af},$$
 (26)

where  $f_d$  is the Doppler shift and a is the Doppler scaling factor. For the underwater cooperative MIMO system, the transmitters have to redo the synchronization and CSI estimation if either the  $SNR < \eta$  or the effective communication time oversteps the coherence time. Therefore, the effective communication time by considering both the SNR and the coherence time can be obtained by:

$$t_{BF} = \operatorname{argmin}\{t_{BF,SNR}, T_c\},\tag{27}$$

and

$$t_{SPTC} = \operatorname{argmin}\{t_{SPTC,SNR}, T_c\}. \tag{28}$$

The efficiency of the underwater cooperative MIMO system can be evaluated by calculating the throughput of the data. By considering the CSI estimation time and synchronization time, an upper bound of the throughput by using beamforming and space-time coding can be respectively written as:

$$Tp_{BF} = \frac{t_{BF}C_{BF}}{\sum_{i=2}^{N} \Delta t_i + t_{CSI} + t_{BF}},$$

$$Tp_{SPTC} = \frac{t_{SPTC}C_{SPTC}}{\sum_{i=2}^{N} \Delta t_i + t_{CSI} + t_{SPTC}},$$
(29)

where  $t_{CSI}$  is the time of the broadcast from the base station for the CSI estimation calculated by:

$$t_{CSI} = \frac{L_{CSI}}{B_{ac}} + \frac{d_{max}}{c_{ac}}. (30)$$

 $L_{CSI}$  is the total packet length delivered for the CSI estimation.  $B_{ac}$  is the bandwidth of the acoustic channel and  $c_{ac}$  is the propagation speed of the acoustic signals.  $d_{max}$  is the maximum distance between the based station and the sensor nodes.  $C_{BF}$  and  $C_{SPTC}$  in (29) are respectively the channel capacity of the cooperative MIMO by using beamforming and space-time coding techniques. By considering the frequency synchronization error, the SNR is not a constant so that the

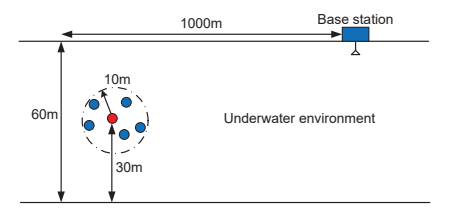


Fig. 7. The geometry of the underwater cooperative MIMO system.

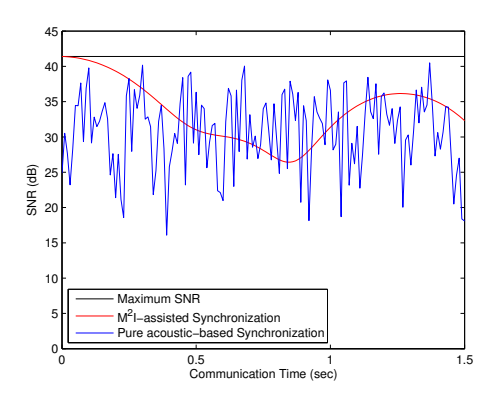


Fig. 8. The SNR of beamforming.

channel capacity varies with the time as well. To calculate the upper bound presented in (29), the maximum SNR obtained at the beginning of the communication can be used and then  $C_{BF}$  and  $C_{SPTC}$  can be expressed as:

$$C_{BF} = \log_2 \left[ \det \left( \mathbf{I}_N + \frac{SNR_{BF,\epsilon}(t=0)}{N_b} \mathbf{H} \mathbf{H}^* \right) \right],$$

$$C_{SPTC} = \log_2 \left[ \det \left( \mathbf{I}_N + \frac{SNR_{SPTC,\epsilon}(t=0)}{N_b} \mathbf{H} \mathbf{H}^* \right) \right],$$
(31)

where  $N_b$  is the number of the base stations. Here we consider one base station so that  $N_b = 1$ .  $\mathbf{I}_N$  is denotes the identity matrix of size N.  $\mathbf{H}$  is the  $N \times N_b$  channel matrix.

#### VI. Numerical Evaluation

In this section, we evaluate the performance of the proposed underwater cooperative MIMO systems by considering the pure acoustic communications and  $M^2I$ -acoustic communications. The geometry of the underwater cooperative MIMO system is considered as Fig. 7. The transmitting power from each transmitter is set to be 10 mW. The power of the noise is  $9.81\times10^{-3}$  mW [14]. The  $M^2I$  transmitters operate at 10 MHz frequency with 20 kHz bandwidth. The acoustic transmitters operate at 10 kHz frequency with 10 kHz bandwidth.

The SNRs of using beamforming and space-time coding are evaluated in Fig. 8 and Fig. 9, respectively. The SNR is calculated for the first 1.5 seconds after completing the synchronization. 5 slave nodes are randomly deployed around a master node within 10 meters range. The black horizontal line is the maximum SNR by considering the perfect time and frequency synchronization. The result of using M<sup>2</sup>I-assisted synchronization is shown as the red curve. At the beginning

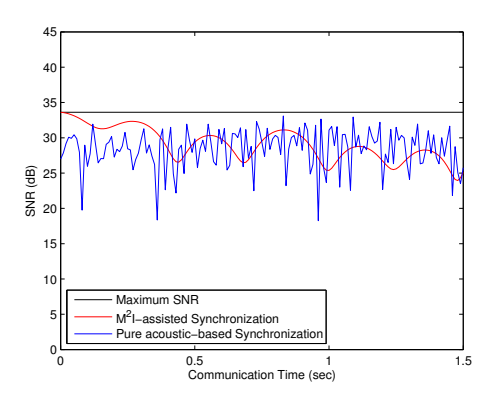


Fig. 9. The SNR of space-time coding.

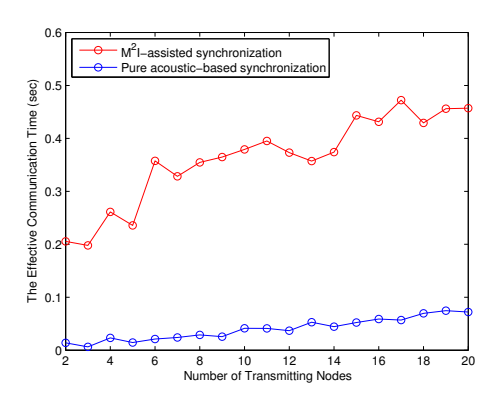


Fig. 10. The effective communication time of beamforming.

t=0, the SNR is very close to the upper bound since the  $\rm M^2I$  can provide very accurate synchronization due to the small delay and larger bandwidth. But it decrease as the time increases and becomes random since the phases are not aligned after a certain time. Shown as the blue curve, the SNR of using pure acoustic-based synchronization randomly varies since the acoustic communication cannot provide the accurate synchronization. The phases cannot be aligned even at the beginning of the communication.

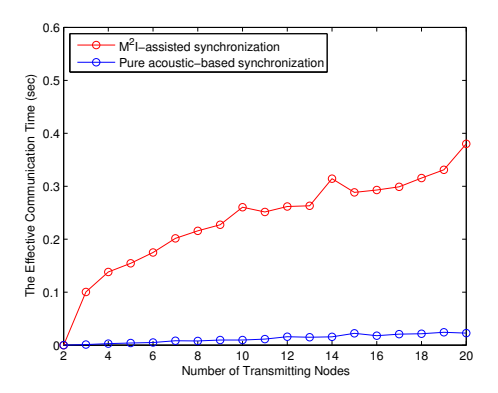


Fig. 11. The effective communication time of space-time coding.

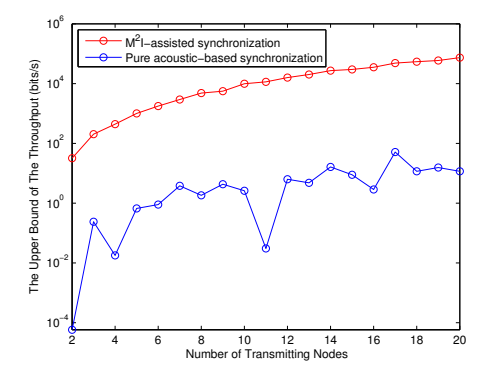


Fig. 12. Upper bound of the throughput by using beamforming techniques.

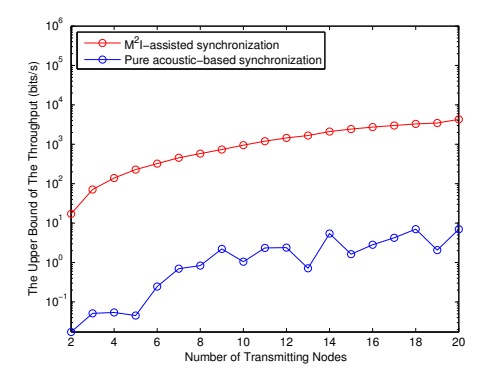


Fig. 13. Upper bound of the throughput by using space-time coding techniques.

The effective communication time in (27) and (28) is evaluated in Fig. 10 and Fig. 11. The threshold of minimum SNR  $\eta = 25$  dB. In this evaluation, the number of transmitting nodes increases from 2 to 20. For each number of transmitting nodes, we randomly deploy the slave nodes for 100 times and calculate the average effective communication time. The effective communication time increases with the number of transmitting nodes increases since the total transmitting power is larger if more nodes are used. However, the effective communication time does not increase monotonically since it takes more time to synchronize more nodes. As a result, the synchronization error becomes larger. Moreover, the randomness of the nodes' deployment also influences the effective communication time. The result shows that the cooperative MIMO system can have more effective communication time if the M<sup>2</sup>I-assisted synchronization is used.

Finally, we calculate an upper bound of the throughput in Fig. 12 and Fig. 13. Compared to the cooperative MIMO system synchronized by acoustic communications, the  $M^2I$  synchronized systems have shorter synchronization time and longer effective communication time. Therefore, the throughput can be enhanced by using  $M^2I$ -assisted synchronization.

#### VII. Conclusion

In this paper, we propose a cooperative M<sup>2</sup>I-acoustic MIMO systems for the communications of underwater robot swarms. To evaluate the performance of the proposed cooperative MIMO system in underwater environments, we first analyze the synchronization accuracy of the distributed transmitters by calculating the time and frequency errors. Based on the synchronization accuracy, we analyze the communication performance by considering beamforming and space-time coding techniques. Compared to the pure acoustic communications, the hybrid M<sup>2</sup>I-acoustic communication paradigm enables more robust underwater cooperative MIMO systems due to the smaller channel delay and the larger bandwidth of the MI techniques. The comparison results, including the SNR, effective communication time, and an upper bound of the throughput, are validated in the numerical evaluation.

#### REFERENCES

- [1] N. E. Leonard, D. A. Paley, R. E. Davis, D. M. Fratantoni, F. Lekien, and F. Zhang, "Coordinated Control of An Underwater Glider Fleet in An Adaptive Ocean Sampling Field Experiment in Monterey," Journal of Field Robotics, vol. 27, No. 6, pp. 718-740, September, 2010.
- [2] D. Paley, Fumin Zhang, and N. E. Leonard, "Coordinated Control for Ocena Sampling: The glider Coordinated Control System," IEEE Transactions on Control System Technology, vol. 16, No. 4, pp. 735-744, July, 2008.
- S. Liu, J. Sun, J. Yu, A. Zhang, and F. Zhang, Sampling Optimization for Networked Underwater Gliders, In Proc. of IEEE/MTS Oceans 2016, Shanghai, China, 2016.
- [4] J. Zhang and Y. R. Zheng, "Frequency-Domain Turbo Equalization with Soft Successive Interference Cancellation for Single Carrier MIMO Underwater Acoustic Communications," IEEE Transactions on Wireless Communications, vol. 10, No. 9, pp. 2872-2882, September, 2011.

  [5] Hamed, Ezzeldin, Hariharan Rahul, Mohammed A. Abdelghany, and Dina
- Katabi, "Real-time distributed MIMO systems," *In Proceedings of the* 2016 ACM SIGCOMM Conference, pp. 412-425, August, 2016.
- [6] H. Guo, Z. Sun, J. Sun, and N. M. Lichinitser, "M2I: Channel Modeling for Metamaterial-Enhanced Magnetic Induction Communications," IEEE Transactions on Antennas and Propagation, vol. 63, No. 11, pp. 5072-5087, November, 2015.
- H. Guo, Z. Sun, and P. Wang, "Channel modeling of MI Underwater Communication Using Tri-Directional Coil Antenna," In Proc. of IEEE Globecom 2015, San Diego, USA, December, 2015
- R. Mudumbai, D. R. Brown Iii, U. Madhow and H. V. Poor, "Distributed transmit beamforming: challenges and recent progress," in IEEE Communications Magazine, vol. 47, no. 2, pp. 102-110, February 2009.
- S. Jayaprakasam, S. K. A. Rahim, and C. Y. Leow, "Distributed and Collaborative Beamforming in Wireless Sensor Networks: Classifications,
- Trends and Research Directions," *IEEE Communications Surveys and Tutorials*, No. 99, pp. 1-26, July, 2017.

  [10] D. R. Brown and H. V. Poor, "Time-Slotted Round-Trip Carrier Synchronization for Distributed Beamforming," *IEEE Transactions on Signal Processing*, vol. 56, No. 11, pp. 5630-5643, November, 2008.
- [11] S. Shi, S. Zhu, X. Gu, and R. Hu, "Extendable carrier synchronization for distributed beamforming in wireless sensor networks," In Proc. of 2016 International Wireless Communications and Mobile Computing Conference (IWCMC), Paphos, Cyprus, September, 2016.
- [12] M. Naderi, M. Patzold, R. Hicheri, and N. Youssef, "A Geometry-Based Underwater Acoustic Channel Model Allowing for Sloped Ocean Bottom Conditions," IEEE Transactions on Wireless Communications, vol. 16, No. 4, pp. 2394-2408, April, 2017.
- [13] T. S. Rappaport, "Wireless Communications: Principles and Practive,"
- New Jersey: Presntice Hall PTR, Upper Saddle River, 2001.
  [14] E. Demirors, G. Sklivanitis, T. Melodia, S. Batalama, and D. Pados, "Software-defined Underwater Acoustic Networks: Towards a High-rate Real-time Reconfigurable Modem," *IEEE Communications Magazine*, vol. 53, No. 11, pp. 64-71, November, 2015.
- [15] H. Kulhandjian, T. Melodia and D. Koutsonikolas, "CDMA-Based Analog Network Coding for Underwater Acoustic Sensor Networks," IEEE Transactions on Wireless Communications, vol. 14, no. 11, pp. 6495-6507,